Materials Science-Poland, 42(1), 2024, pp. 52-61
http://www.materialsscience.pwr.wroc.pl/
DOI: 10.2478/msp-2024-0004

Enhanced catalytic activity of zeolitic imidazolate frameworks (ZIF-8) polyelectrolyte complex composites membranes by laser etching

Ting Yu[1], Boonyarach Kitiyanan[1,2], Stephan Thierry Dubas[1,2,*]

[1]The Petroleum and Petrochemical College, Chulalongkorn University, Bangkok 10330, Thailand
[2]Center of Excellence on Petrochemical and Materials Technology, Bangkok 10330, Thailand

The effect of laser etching on the surface properties of composite polyelectrolyte complex (PEC) based membranes as mixed matrix membranes was studied. The PECs were prepared by the stoichiometric mixing of cationic PDDA (poly(diallyl dimethyl ammonium chloride)) and anionic PSS (poly(sodium 4-styrene sulfonate)) as polyelectrolytes with various contents of ZIF-8 as filler. Composite membranes usually display improved bulk properties depending on the nature of the filler, but the surface properties are often dictated by the matrix covering the surface. The PEC composite membranes were then subjected to laser etching, resulting in the enhanced exposure of embedded ZIF-8 particles within the PEC structure in an attempt to improve the surface properties of the composite membrane. The crystal structure, morphology, and distribution of zinc at the PECs surface, before and after laser etching, were characterized using X-ray diffraction (XRD), field emission scanning electron microscopy (FE-SEM), and energy-dispersive X-ray spectroscopy (EDS), respectively. In order to evaluate the improvement of the surface properties of the laser-etched membranes, a model experiment involving a catalytic reaction was chosen. The pristine and laser treated surfaces were tested for their catalytic activity for the transesterification of triglycerides present in soybean oil with methanol at a temperature of 150°C. Interestingly, the laser-etched PECs displayed substantially enhanced activity compared to the original composite PEC membranes as a result of surface erosion. These results could be interesting for the future development of composite membranes with improved surface properties where the filler needs to expose the surface of the membranes.

Keywords: *PECs, ZIF-8, laser, etching*

1. Introduction

Polyelectrolyte complexes (PECs) are formed by the complexation of oppositely charged polyelectrolytes in a solution that is primarily driven by electrostatic interactions between water-soluble polyelectrolytes. Hydrogen bonding and hydrophobic interactions can also influence the final structure of PECs [1, 2]. PECs can be found in diverse applications such as drug delivery, biosensing, battery separators, fuel cells, and catalysis [3–7]. PDDA, a cationic polyelectrolyte, and PSS, an anionic polyelectrolyte, are often used to prepare PECs. These two polyelectrolytes can form strong complexes, but the addition of salt during the formation of PECs can swell the PDDA/PSS membranes, increasing their thickness and improving their plasticity [8]. Notably, one significant advantage of PDDA/PSS PECs is their excellent stability against dissolution in most organic solutions [9, 10]. PDDA/PSS PECs can be used as a matrix for the immobilization of various fillers such as conducting particles (carbon black), redox species (MnO2), or even catalytic particles such as metal-organic frameworks [11–13]. The filler, which is usually found inside the membranes, has limited access to the solution, thus reducing the interaction between the filler particle and the solution if needed, for example, for catalytic particles. A possible solution is to use an etching step to erode the surface of the membrane and expose the particle within.

Laser etching is a proven technology used to remove material from a substrate using a

* E-mail: Stephan.d@chula.ac.th

© Ting Yu et al. 2024. This is an open access article distributed under the Creative Commons Attribution-NonCommercial-NoDerivatives 4.0 License. (http://creativecommons.org/licenses/by-nc-nd/4.0/)

high-energy laser beam [14]. Although chemical etching has a lower upfront investment cost and a higher production efficiency, industries such as the glass, plastic, semiconductor, and steel industries [15–18] are increasingly focused on laser etching strategies because of their lower comprehensive cost, precise engraving, and greater environmental friendliness due to zero waste emission [19–22]. While the etching of a polymer surface can be used to induce the formation of chemical structures or erode the surface [23, 24], the etching of polyelectrolyte complexes, although never reported yet, could be of great interest to modify the membrane interface. The need for surface treatment comes from the fact that after compression molding, the membranes are very smooth, and the particles are entrapped within the membranes with limited access to the surface. The particle's limited access to the surface is the result of the processing method in which heat and pressure to the polymer-filler mixture promote the flow and redistribution of the polymer matrix around the filler particles. As a result, the particles become encapsulated within the matrix rather than being pushed to the surface. This could be interesting, for example, in applications where roughness and high surface area are needed between the electrolyte and the membrane, especially for catalytic surface or solvent and ion transport through the membrane.

To study the effect of laser etching, a composite PEC films were prepared by combining PDDA/PSS as a matrix with oxidized ZIF-8 powder rich in N=C=O bonds that are known to enhance the conversion of triglycerides [25, 26]. Laser etching was employed to erode the PECs and expose the ZIF-8 from the interior of the membrane. The hypothesis in this work was that the laser could etch the PEC surface and, therefore, expose the inner particles. The PECs were characterized using X-ray diffraction (XRD), field emission scanning electron microscopy (FE-SEM), and energy-dispersive X-ray spectroscopy (EDS). Furthermore, the performance of the catalytic PECs was evaluated in the transesterification of triglycerides found in soybean oil, which is an important reaction to synthesize fatty acid methyl ester (FAME), the main component of biodiesel, as a model experiment.

2. Experimental

2.1. Materials

Poly(diallyldimethylammonium chloride) (PDDA) (Mw=200,000-350,000, 20 wt% in H2O) are purchased from Sigma-Aldrich. Poly(sodium 4-styrenesulfonate) (PSS) (Mw=70,000) is provided by ACROS. Sodium chloride is supplied by Pine Chemical Co., Ltd. Zinc Nitrate Hexahydrate (98%) and 2-Methylimidazole (99%) were obtained from Sigma-Aldrich. Methanol ($\geq$99.9%) was bought from Fisher Chemical. All chemical reagents are analytical grade purity. Soybean oil was purchased by Thai Vegetable Oil Public Company Limited.

2.2. Synthesis of ZIF-8

ZIF-8 was prepared according to Janosch Cravillon's report with few modifications [27]. 7.0 mmol $Zn(NO_3)_2$ and 56.0 mmol 2-Methylimidazole (Zinc : 2-Methylimidazole = 1:8) were dissolved in 200 mL methanol. Then, $Zn(NO_3)_2$ solution was added into 2-methylimidazole solution quickly. After vigorous stirring of 16 hours at room temperature, the ZIF-8 solid was separated by centrifugation machine (10000 rmp, 30 min) and washed with excess methanol three times. White ZIF-8 solid was dried in a vacuum oven at 60°C overnight to evaporate methanol. The above ZIF-8 was oxidized in the furnace at 300°C for 3 hours in the air.

2.3. Formation of PECs of xZIF/PEC

The ZIF-8 was added to a mixture solution of PDDA/NaCl (PDDA: 0.1 mol/L, NaCl: 1 mol/L). The mixture was sonicated for 15 minutes to disperse ZIF-8 in the PDDA/NaCl solution. The PDDA/NaCl/ZIF-8 solution was combined with an equal volume of PSS/NaCl solution (PSS: 0.1 mol/L, NaCl: 1 mol/L) and stirred slowly for five minutes. The resulting primary solid of PECs was obtained and isolated by vacuum filtration. The primary solid of the PECs was compressed using a compressor at a pressure of 2000 psi and a temperature of 60°C for 10 minutes. The resulting ZIF-8/PDDA/PSS was dried at room temperature

until the moisture had evaporated, and it was called xZIF/PEC. Here, x represents the weight fraction of ZIF-8 in the PDDA/PSS membrane.

2.4. Laser etching of xZIF/PEC

The untreated xZIF/PEC samples were etched by a 500 mW laser (wavelength: 405 nm). The engraving parameters were a density of 10 lines/mm at a speed of 800 mm/min. These samples were noted as xZIF/PEC-L, with x representing the weight fraction of ZIF-8 in the matrix and L denoting the laser treatment.

2.5. Measurement of the catalytic efficiency

A transesterification reaction was used as an example to test the performance of catalytic PECs in the batch reactor. The schematic of the batch reactor and photograph of the batch reactor are provided in Fig. S1 in the supporting materials section. Catalytic PECs, 3 wt% of soybean oil, were added into 72.5 mL soybean oil and 17.4 mL methanol mixture (mole ratio of soybean oil and methanol was 1:6). A sealed batch reactor with a magnetic stirrer was heated in oil bath on 150°C for 4 hours. After the reaction, the PECs were isolated from the product by vacuum filtration. The excess methanol in the product was evaporated off in a rotary evaporator under negative pressure. The product was separated into a FAME mixture and glycerol by gravity using a separatory funnel.

2.6. Catalytic PECs characterization

X-ray diffraction (XRD) patterns were acquired using a Rigaku SmartLab instrument (Japan) equipped with Cu-Kα radiation ($\lambda = 1.542$ Å) and operated at 40 kV and 30 mA. The relative intensities were recorded in the range of 5–40° at a scanning rate of 5°/min. Field emission scanning electron microscope (FE-SEM) images were obtained utilizing a Hitachi S4800 FE-SEM (Japan) equipped with energy-dispersive X-ray spectroscopy (EDS).

2.7. Analysis of FAME product

The conversion of triglyceride was analyzed by high-performance liquid chromatography (HPLC) using a CTO-10AS VP instrument and an Agilent Eclipse XDB-C18 column, both manufactured by Shimadzu. The FAME mixture was diluted with acetone, and the 20 μL sample was injected into HPLC. The conversion of triglycerides was calculated by the following expression:

$$C_{tg} = \frac{Consumed\ triglycerides}{Total\ triglycerides} \times 100\%$$

where C_{tg} is the conversion of triglyceride. The examples of HPLC chromatograms are presented in Fig. S2.

The yield of fatty acid methyl ester (FAME) was calculated by the following expression:

$$Y_{FAME} = \frac{W_{FAME}}{W_{oil}} \times 100\%$$

where Y_{FAME} is yield of FAME in the product, W_{FAME} is total weight of FAME, and W_{oil} is weight of soybean oil used in the reaction. The total weight of FAME was analyzed by Agilent 7820A gas chromatography (GC) using DB-Fast FAME column. Supelco 37 component FAME mix (Sigma-Aldrich) was used as the calibration standard. The reaction product was diluted with toluene and 1μL sample was injected into GC. The examples of GC chromatograms are presented in Fig. S3.

3. Results and discussion

The initial step in this study was the synthesis of ZIF-8 and oxidized ZIF-8, which were characterized by X-ray diffraction (XRD), and the corresponding data are presented in Figure 1(a). The observed relative peaks, including 011, 002, 112, 022, 013, 222, 114, 233, and 131, are in good agreement with previous reports, confirming the successful synthesis of ZIF-8 with a sodalite structure [28–30]. The crystallinity of the ZIF-8 was significantly improved after oxidation, as indicated by the higher intensity of each peak (XRD spectra are available in the supporting document section). Figure 1(b) shows the field emission scanning electron microscopy (FE-SEM) images of the oxidized

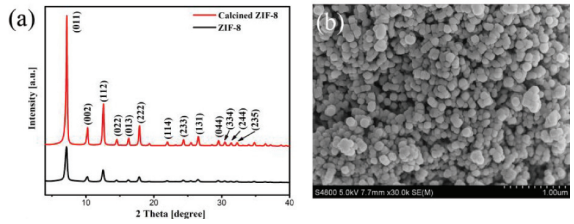

Fig. 1. (a) XRD patterns of ZIF-8 and calcined ZIF-8, (b) FE-SEM images of calcined ZIF-8

ZIF-8, revealing an average particle diameter of approximately 150 nm, which facilitates their dispersion in aqueous solutions.

The formation of ZIF/PECs occurs spontaneously through the complexation process of the PDDA, and PSS, driven by the association between opposite charges [31]. The ZIF-8 were initially dispersed in a PDDA solution due to their anionic character, resulting in the formation of the ZIF/PDDA mixture. Subsequently, the addition of PSS enables electrostatic interactions between PDDA and PSS, leading to the formation of the composite PECs with the ZIF-8. During the formation process, increasing ZIF-8 content tends to increase the stiffness and roughness of the PECs, as shown in the pictures in Figure 2. A smooth and transparent PEC membrane was prepared without the addition of ZIF-8 (0ZIF/PEC), while the incorporation of increasing amount of ZIF-8 led to the formation of a rough and brown xZIF/PEC. When compared to the soft and flexible PDDA/PSS PECs, the increasing content of ZIF-8 filler led to a harder and more brittle composite.

As mentioned in the introduction, the main problem with composite materials is that the filler can hardly be accessible to the surface, which is a limiting factor for the utilization of reactive and catalytic particles. Here, to expose more ZIF-8 from the PECs during transesterification, a laser was used to erode the surface of the sample. As shown in Figure 3, engraving marks after laser are noticeable on the surface of the etched samples, while the surface of the PECs before etching was smooth, and shimmy appears rough and dull after etching.

On the FE-SEM images in Figure 4, the morphology of each (0-90)ZIF/PEC after laser etching is visible. The scratches on the surface of 0ZIF/PEC-L are hardly noticeable because the transparent PEC lets the laser pass through, and almost none of the laser energy is absorbed by the sample. Similarly, only faint scratches can be seen on the surface of 10ZIF/PEC for the same reason. Nevertheless, when more than 30wt% of ZIF-8 was added to the PECs, a clear laser marking was visible on the surface of the samples. From image analysis, it can be calculated that the path of the laser for etching covers around 28% of the surface of the PECs (The calculation method is presented in supporting materials and Fig. S4). The etching lines could not be made in a tighter pattern due to the limitation of the stepper motor used to control the displacement of the laser.

The distribution of ZIF-8 at the PECs surface after laser etching was analyzed by SEM with the EDS mapping mode, as presented in Figure 5. The Zinc element was chosen to be detected because only ZIF-8 contains Zn. Results demonstrate that a higher concentration of Zn is detected in the area etched by laser for samples containing more than 50 wt% ZIF-8, particularly 90ZIF/PEC-L, while a lower concentration is found in the area without laser etching. This indicates that during the compression process, ZIF-8 flows within the polymer PECs due to the surface energy and interaction between the polymers and ZIF-8. A laser with high energy can ablate the polymer surface and expose the ZIF-8 inside the PECs to the reactants, resulting in improved catalytic activity. A similar trend is observed in 30ZIF/PEC-L, but to a lesser extent due to the lower initial concentration of ZIF-8. In conclusion, despite being covered by PDDA/PSS during the preparation process of PECs, the surface of PECs can be etched by laser to reveal more ZIF-8 and improve the catalytic activity of the reaction.

The XRD patterns of the samples before and after laser etching are presented in Figure 6. The patterns of 70ZIF/PEC and laser-ablated 70ZIF/PEC illustrate that almost no structural transformation occurred, demonstrating that ZIF-8 could maintain its complete crystal structure under laser etching, thus ensuring its catalytic activity during the reaction.

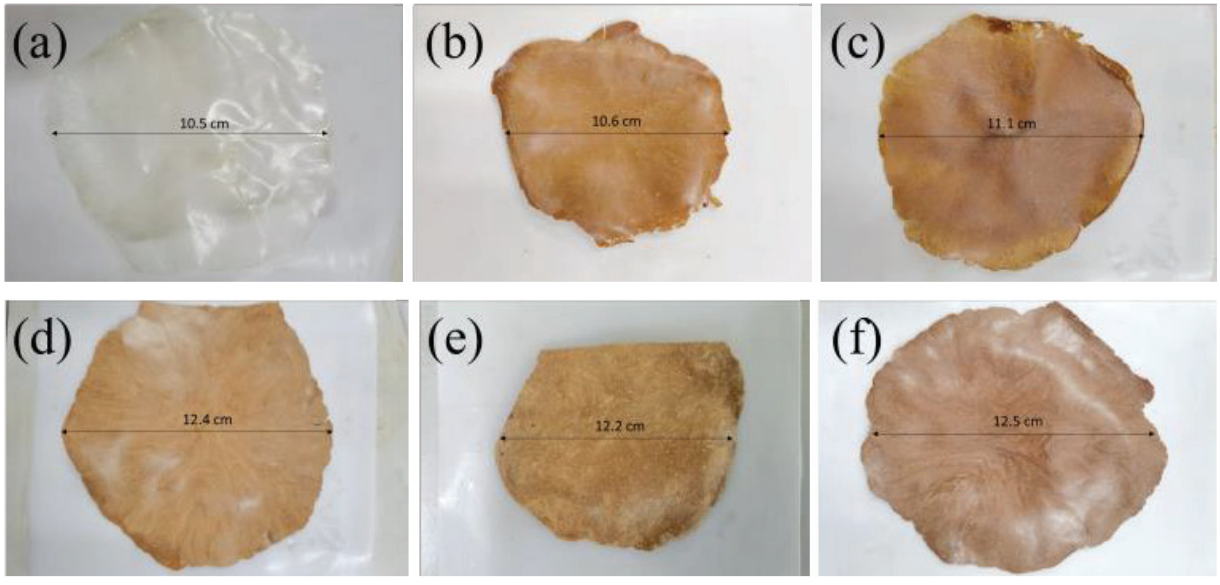

Fig. 2. Pictures of PECs that (a) 0ZIF/PEC, (b) 10ZIF/PEC, (c) 30ZIF/PEC, (d) 50ZIF/PEC, (e) 70ZIF/PEC and (f) 90ZIF/PEC



Fig. 3. Photo of PECs before (left side) and after (right side) laser etching

Figure 7 shows the ATR-FTIR spectra of samples before and after lasing etching. In the spectra of PDDA, peaks observed at 3384 cm^{-1} and 1640 cm^{-1} are attributed to $–NR^{3+}$ stretching vibration and –NH deformation vibration, and peaks around 2924 cm^{-1} and 1462 cm^{-1} are associated with C–H bending vibrations of [32]. In addition, peaks of PSS observed at 1040 cm^{-1} and 1005 cm^{-1} are designated as symmetric and asymmetric stretching vibrations of the sulfonate groups [32, 33]. For 70ZIF/PEC and 70ZIF/PEC-L samples, the peak at 755 cm^{-1} is attributed to the C-H bending of ZIF-8, and the peak at 1138 cm^{-1} is associated with the C–N stretch of ZIF-8 [34, 35]. The intensity of the characteristic peaks of ZIF-8 in 70ZIF/ PEC-L is stronger than that in 70ZIF/PEC, demonstrating that more ZIF-8 powder is exposed from the polymer of PDDA and PSS after laser etching. Noteworthy, peaks of 70ZIF/PEC and 70ZIF/PEC-L remained unchanged, indicating that there is no change in the chemical structure of PECs after laser etching.

To ensure that the ZIF-8 powder exposed to laser (ZIF-8-L) had similar catalytic efficiency as the original ZIF-8, both powders were used to catalyze triglycerides in soybean oil (Fig. S5). The reaction rate and final conversion of ZIF-8-L were similar to those of ZIF-8, demonstrating that ZIF-8 remained active after being exposed to the laser. This result, along with the XRD pattern (Fig. 6), indicates that the laser had negligible influence on ZIF-8.

The yield of FAME and stability of the catalysts while being used in up to 5 cycles is shown in Fig. 8. Obviously, high yield can be achieved by 90ZIF/PEC-L and 70ZIF/PEC-L, and their activity decreased almost linearly after reusing the catalysts several times. Among all the xZIF/PEC catalysts,

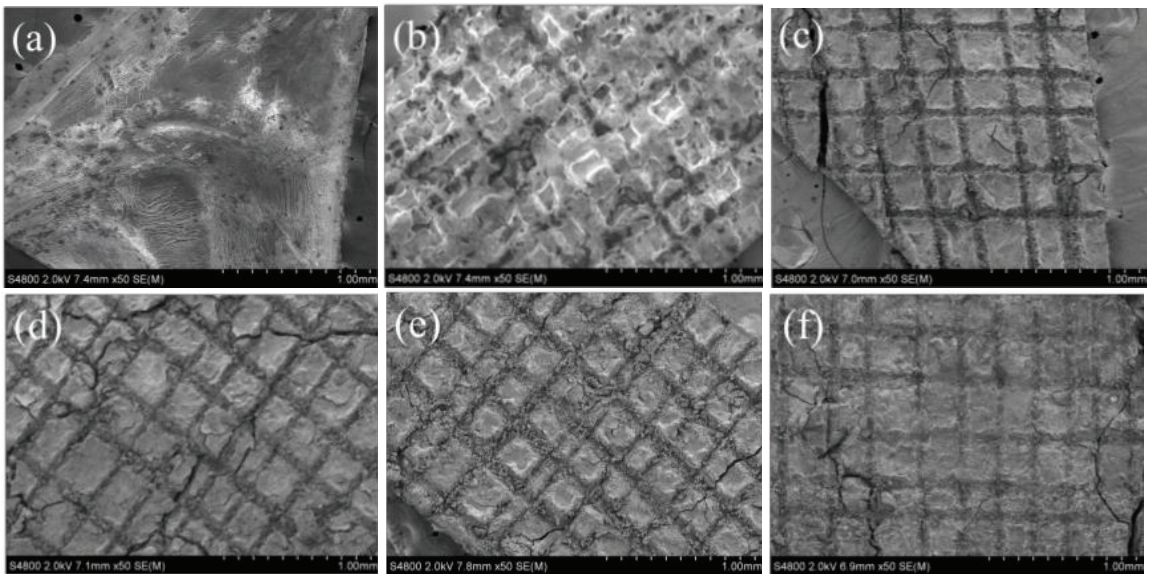

Fig. 4. FE-SEM images of (a) 0ZIF/PEC-L, (b) 10ZIF/PEC-L, (c) 30ZIF/PEC-L, (d) 50ZIF/PEC-L, (e) 70ZIF/PEC-L, and (f) 90ZIF/PEC-L

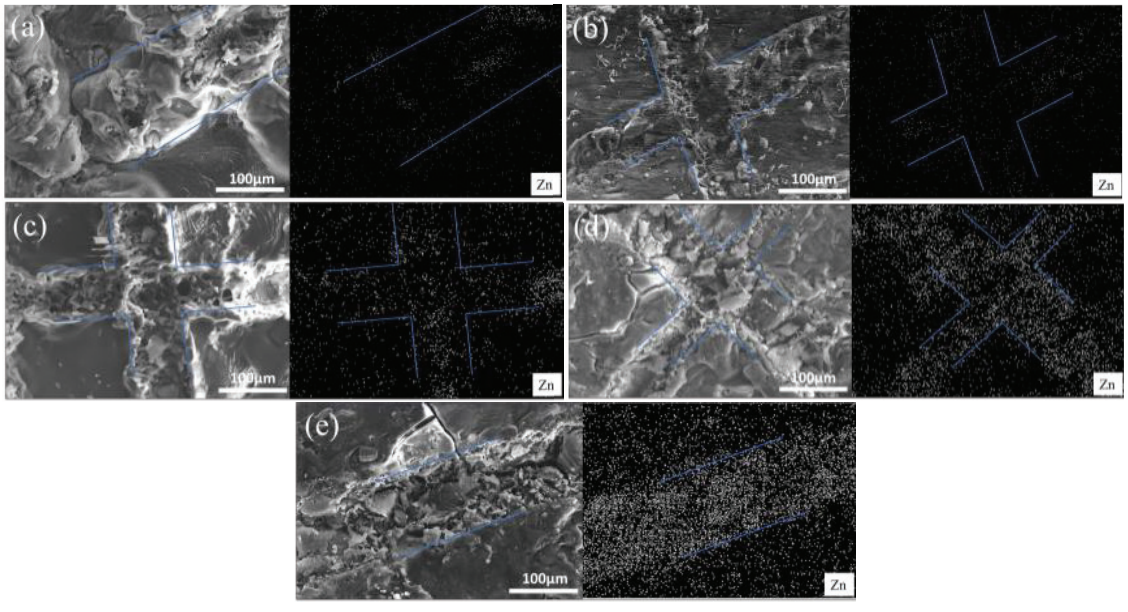

Fig. 5. FE-SEM images of xZIF/PEC etched by laser (left side) and corresponding EDS mapping of Zn distribution (right side): (a) 10ZIF/PEC-L, (b) 30ZIF/PEC-L, (c) 50ZIF/PEC-L, (d) 70ZIF/PEC-L and (e) 90ZIF/PEC-L

90ZIF/PEC-L presented the best yield, but due to excessive brittleness, the catalyst appeared to break into small parts, which made it harder to collect at the end of the reaction. Considering both activity and mechanical strength, the 70ZIF/PEC-L would be a better choice as the membranes were able to maintain physical integrity while providing sufficient catalytic activity.

Therefore, PECs with 70% ZIF-8 were chosen for the comparative analysis of reaction activity before and after laser etching, as shown in Figure 9. The conversion of triglyceride using 70ZIF/PEC-L

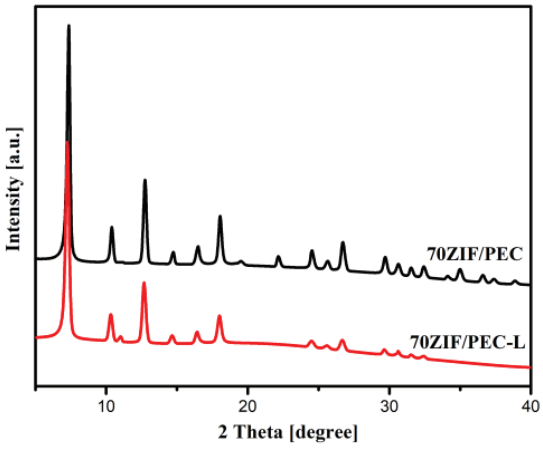

Fig. 6. XRD patterns of 70ZIF/PEC before and after laser etching

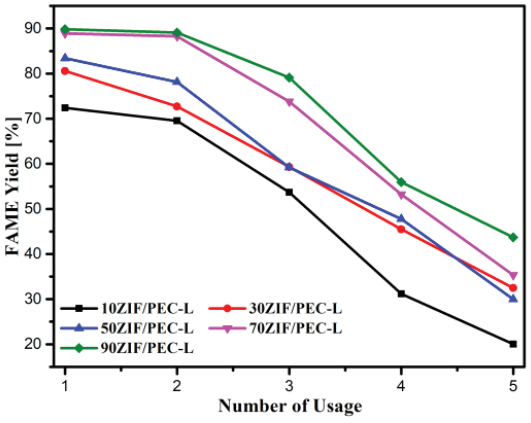

Fig. 8. Triglyceride conversion catalyzed by ZIF/PEC-L with 10%, 30%, 50%, 70%, and 90% ZIF-8 loadings over five times usages

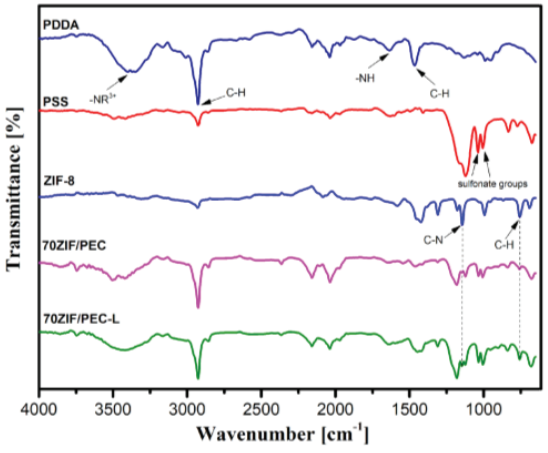

Fig. 7. ATR-FTIR spectra of PDDA, PSS, ZIF-8, 70ZIF/PEC, and 70ZIF/PEC-L

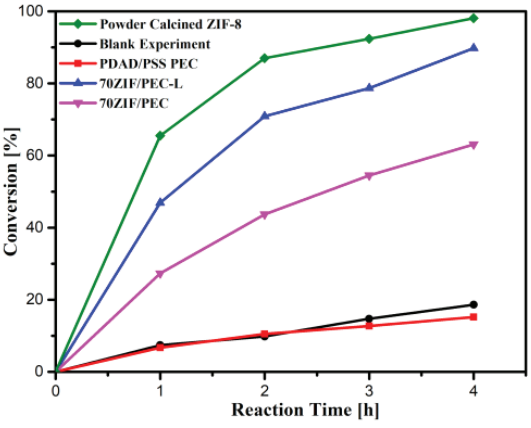

Fig. 9. Conversion of triglyceride in soybean oil by powder calcined ZIF-8, PDDA/PSS PEC, 70ZIF/PEC, 70ZIF/PEC-L, and blank experiment

reached 90%, which is just slightly lower than the ZIF-8 powder but is known to be hard to collect at the end of the reaction, while 70ZIF/PEC reached only 63% conversion of triglyceride. Given that triglycerides undergo catalysis at the active sites on the ZIF-8 surface, augmenting the ZIF-8 content and employing laser etching proves advantageous in exposing more ZIF-8 to reactants, thereby facilitating enhanced mass transfer of molecules from the mixed solution to the active sites. In a similar conversion experiment, pure PDDA/PSS PECs do not have a catalytic function on the reaction, as manifested by a reaction rate similar to the blank experiment.

4. Conclusions

In this research, we have successfully fabricated catalytic PECs by employing oxidized ZIF-8 as the active material. The application of laser etching to expose ZIF-8 particles within the PECs has been demonstrated as an effective strategy to enhance their catalytic activity without compromising their structural integrity. The catalytic performance of these materials was assessed in the transesterification of triglycerides in soybean oil conversion rates. When considering both the catalytic performance and the mechanical stability of the membrane, the

70ZIF/PEC-L sample provided the best conversion while maintaining physical integrity of the membrane during the transesterification reaction. This work presents an innovative approach to catalytic PEC development, with potential applications in biodiesel production and other catalytic processes. The combination of PECs and laser etching opens up new possibilities for designing highly efficient and mechanically robust membranes with superior surface properties.

Acknowledgments

This Research was funded by the Innovation Fund Chulalongkorn University (CU_FRB65_ind (20)_206_63_07) and the Natural Science Foundation of Guizhou Province ([2017]7089).

Supporting Materials

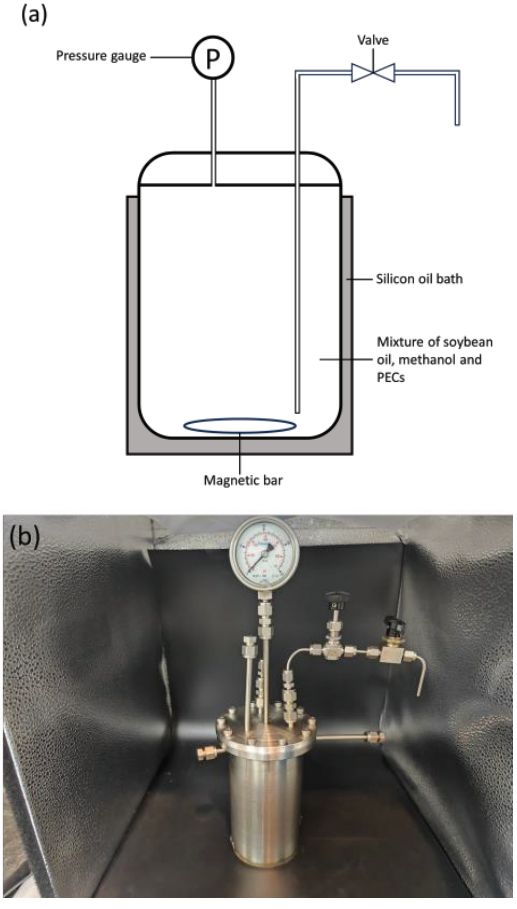

Fig. S1. (a) The schematic of batch reactor for transesterification, and (b) Photograph of batch reactor for transesterification

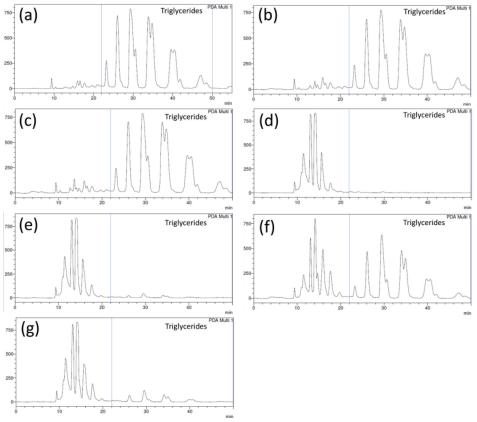

Fig. S2. HPLC chromatograms of (a) soybean oil, FAME converted from soybean oil by (b) no catalyst under 150°C for 4 hours, (c) PDAD/PSS PECs under 150°C for 4 hours, (d) calcined ZIF-8 under 150°C for 4 hours, (e) ZIF-8-L under 150°C for 4 hours, (f) 70ZIF/PEC under 150°C for 4 hours, (g) 70ZIF/PEC-L under 150°C for 4 hours. The conditions of HPLC: an Inertsil ODS-4 column (250 mm $\times$ 4.6 mm $\times$ 5 μm) and a mixture mobile phase consisting of acetone/acetonitrile (80:20 V/V) was used at an oven temperature of 30°C, a flow rate of 0.3 mL/min and a UV wavelength of 205 nm [1].

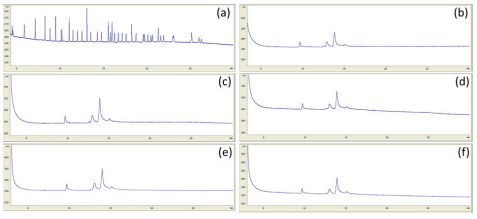

Fig. S3. GC chromatograms of (a) Supelco 37 component FAME mix (C4:0, C6:0, C8:0, C10:0, C11:0, C12:0, C13:0, C14:0, C15:0, C17:0, C18:0, C20:0, C21:0, C22:0, C23:0, C24:0 C14:1, C15:1, C16:1, C17:1, trans-C18:1, cis-C18:1, C20:1, C22:1, C24:1, trans-C18:2, cis-C18:2, C18:3n6, C18:3n3, C20:2, C20:3n6, C2:4n6, C20:3n3, C20:5n3, C22:2n6, C22:6), FAME converted from soybean oil by (b) 10ZIF/PEC-L under 150°C for 4 hours, 1st usage (c) 30ZIF/PEC-L under 150°C for 4 hours, 1st usage (d) 50ZIF/PEC-L under 150°C for 4 hours, 1st usage (e) 70ZIF/PEC-L under 150°C for 4 hours, 1st usage, (e) 90ZIF/PEC-L under 150°C for 4 hours, 1stusage

Calculation method of laser etching

The calculation method of percentage of laser etching is presented as follows. A rectangle area (blue rectangle in Fig. S1) along the middle of the laser notches was chosen as an example for calculation. The increment percentage of surface:

$$R = \frac{S_l - S_r}{S_r} \times 100$$

S_l: surface area after laser etching. S_r: surface area before laser etching.

The calculation formula of S_r:

$$S_r = ab$$

a: length of rectangle. b: height of rectangle.

The calculation formula of S_l:

$$S_l = a\pi r + \pi r(b-2r) + (a-2r)(b-2r)$$

r: radius of laser nicks.

The final calculation demonstrates that the surface area after laser etching is up by 27.7%.

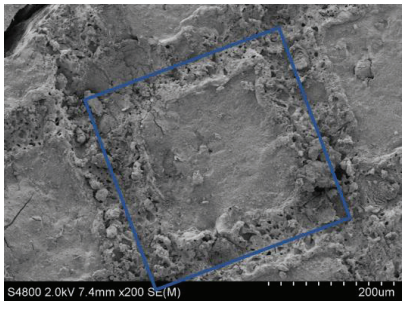

Fig. S4. FE-SEM image of 70ZIF/PEC after laser etching

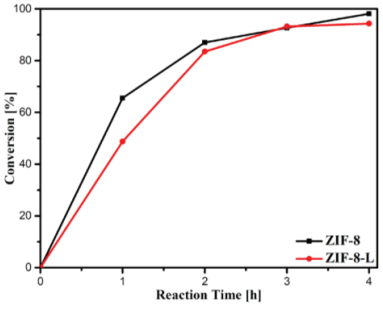

Fig. S5. Conversion of triglyceride in soybean oil by ZIF-8 and ZIF-8 exposed to laser

References

[1] Li L, Srivastava S, Meng S, Ting JM, Tirrell MV. Effects of non-electrostatic intermolecular interactions on the phase behavior of pH-sensitive polyelectrolyte complexes. *Macromolecules.* 2020; 53(18): 7835–7844.

[2] Adhikari S, Leaf MA, Muthukumar M. Polyelectrolyte complex coacervation by electrostatic dipolar interactions. *J Chem Phys.* 2018; 149(16): 163308.

[3] Nikolova D, Simeonov M, Tzachev C, Apostolov A, Christov L, Vassileva E. Polyelectrolyte complexes of chitosan and sodium alginate as a drug delivery system for diclofenac sodium. *Polym Int.* 2022; 71(6): 668–678.

[4] Ivanov A, Davletshina R, Sharafieva I, Evtugyn G. Electrochemical biosensor based on polyelectrolyte complexes for the determination of reversible inhibitors of acetylcholinesterase. *Talanta.* 2019; 194: 723–730.

[5] Debbarma L, Panwar V, Khanduri P, Panwar LS. Development of flexible PVDF/PAMPS polyelectrolyte proton conductive membrane. *Mater Today: Proc.* 2020; 26: 1776–1779.

[6] Zhao Q, An QF, Ji Y, Qian J, Gao C. Polyelectrolyte complex membranes for pervaporation, nanofiltration and fuel cell applications. *J Membr Sci.* 2011; 379(1-2): 19–45.

[7] Luo J, Shi C, Qian X, Zhou K. Novel design and synthesis of bio-based polyelectrolyte complexes for enhancing the flame retardancy of epoxy resin. *Mater Chem Phys.* 2022; 291: 126674.

[8] Dubas ST, Schlenoff JB. Swelling and smoothing of polyelectrolyte multilayers by salt. *Langmuir.* 2001; 17(25): 7725–7727.

[9] Dautzenberg H, Kriz J. Response of polyelectrolyte complexes to subsequent addition of salts with different cations. *Langmuir.* 2003; 19(13): 5204–5211.

[10] Zelner M, Jahn P, Ulbricht M, Freger V. A mixed-charge polyelectrolyte complex nanofiltration membrane: Preparation, performance and stability. *J Membr Sci.* 2021; 636: 119579.

[11] Li Z, Wang J, Liu X, Liu S, Ou J, Yang S. Electrostatic layer-by-layer self-assembly multilayer films based on graphene and manganese dioxide sheets as novel electrode materials for supercapacitors. *J Mater Chem.* 2011; 21(10): 3397–3403.

[12] Teng X, Yu C, Wu X, Dong Y, Gao P, Hu H, et al. PTFE/SPEEK/PDDA/PSS composite membrane for vanadium redox flow battery application. *J Mater Sci.* 2018; 53: 5204–5215.

[13] Shutava T, Jansen C, Livanovich K, Pankov V, Janiak C. Metal organic framework/polyelectrolyte composites for water vapor sorption applications. *Dalton Trans.* 2022; 51(18): 7053–7067.

[14] Houle FA. Basic mechanisms in laser etching and deposition. *Appl Phys A.* 1986; 41: 315–330.

[15] Dalaq AS, Barthelat F. Three-Dimensional Laser Engraving for Fabrication of Tough Glass-Based Bioinspired Materials. *JOM.* 2020; 72(4): 1487–1497. doi: 10.1007/s11837-019-04001-w

[16] Gabriel EFM, Coltro WKT, Garcia CD. Fast and versatile fabrication of PMMA microchip electrophoretic devices by laser engraving. *Electrophoresis.* 2014; 35(16): 2325–2332. doi: 10.1002/elps.201300511

[17] Pavithra B, Prabhu SG, Nayak MM. Design, development, fabrication, and testing of low-cost, laser-engraved, embedded, nano-composite-based pressure sensor. *ISSS J Micro Smart Syst.* 2022; 11(2): 349–353. doi: 10.1007/s41683-021-00076-3

[18] Yang Z, Li W, Liu S, Gao Q. Study on overlap rate and machinability of selected laser melting of maraging steel. *Mater Sci-Pol.* 2023; 41(2): 368–382.

[19] Li Y, Fischer R, Zboray R, Boillat P, Camenzind M, Toncelli C, et al. Laser-engraved textiles for engineering capillary flow and application in microfluidics. *ACS Appl Mater Interfaces.* 2020; 12(26): 29908–29916.

[20] Konstantinou G, Chil R, Desco M, Vaquero JJ. Subsurface laser engraving techniques for scintillator crystals: methods, applications, and advantages. *IEEE Trans Radiat Plasma Med Sci.* 2017; 1(5): 377–384. doi: 10.1109/TRPMS.2017.2714265.

[21] Wang M, Yang Y, Gao W. Laser-engraved graphene for flexible and wearable electronics. *Trends Chem.* 2021; 3(11): 969–981. doi: 10.1016/j.trechm.2021.09.001

[22] Pungjunun K, Yakoh A, Chaiyo S, Praphairaksit N, Siangproh W, Kalcher K, et al. Laser engraved microapillary pump paper-based microfluidic device for colorimetric and electrochemical detection of salivary thiocyanate. *Microchem Acta.* 2021; 188(4): 140. doi: 10.1007/s00604-021-04793-2.

[23] Vivaldi FM, Dallinger A, Bonini A, Poma N, Sembranti L, Biagini D, et al. Three-dimensional (3D) laser-induced graphene: structure, properties, and application to chemical sensing. *ACS Appl Mater Interfaces.* 2021; 13(26): 30245–30260.

[24] Ravi-Kumar S, Lies B, Zhang X, Lyu H, Qin H. Laser ablation of polymers: A review. *Polym Int.* 2019; 68(8): 1391–1401.

[25] Wang T, Wang Y, Sun M, Hanif A, Wu H, Gu Q, et al. Thermally treated zeolitic imidazolate framework-8 (ZIF-8) for visible light photocatalytic degradation of gaseous formaldehyde. *Chem Sci.* 2020; 11(26): 6670–6681. doi: 10.1039/D0SC01397H

[26] Canilho N, Jacoby J, Pasc A, Carteret C, Dupire F, Stébé MJ, et al. Isocyanate-mediated covalent immobilization of Mucor miehei lipase onto SBA-15 for transesterification reaction. *Colloids Surf, B.* 2013; 112: 139–145. doi: 10.1016/j.colsurfb.2013.07.024

[27] Cravillon J, Schröder CA, Bux H, Rothkirch A, Caro J, Wiebcke M. Formate modulated solvothermal synthesis of ZIF-8 investigated using time-resolved in situ X-ray diffraction and scanning electron microscopy. *CrystEngComm.* 2012; 14(2): 492–498. doi: 10.1039/C1CE06002C.

[28] Kaur H, Mohanta GC, Gupta V, Kukkar D, Tyagi S. Synthesis and characterization of ZIF-8 nanoparticles for controlled release of 6-mercaptopurine drug. *J Drug Delivery Sci Technol.* 2017; 41: 106–112. doi: 10.1016/j.jddst.2017.07.004

[29] Beh JJ, Lim JK, Ng EP, Ooi BS. Synthesis and size control of zeolitic imidazolate framework-8 (ZIF-8): From the perspective of reaction kinetics and thermodynamics of nucleation. *Mater Chem Phys.* 2018; 216: 393–401. doi: 10.1016/j.matchemphys.2018.06.022

[30] Ta DN, Nguyen HKD, Trinh BX, Le QTN, Ta HN, Nguyen HT. Preparation of nano-ZIF-8 in methanol with high yield. *Can J Chem Eng.* 2018; 96(7): 1518-1531. doi: 10.1002/cjce.23155

[31] De Geest BG, Jonas AM, Demeester J, De Smedt SC. Glucose-responsive polyelectrolyte capsules. *Langmuir.* 2006; 22(11): 5070–5074.

[32] Zhang W, Wu L, Du L, Yue L, Guan R, Zhang Q, et al. Layer-by-layer assembly modification to prepare firmly bonded Si–graphene composites for high-performance anodes. *RSC Adv.* 2016; 6(6): 4835–4842.

[33] Gui Z, Du B, Qian J, An Q, Zhao Q. Construction and deconstruction of multilayer films containing polycarboxybetaine: Effect of pH and ionic strength. *J Colloid Interface Sci.* 2011; 353(1): 98–106.

[34] Zhang H, Zhao M, Yang Y, Lin YS. Hydrolysis and condensation of ZIF-8 in water. *Microporous and Mesoporous Materials.* 2019; 288: 109568.

[35] Jing H-P, Wang C-C, Zhang Y-W, Wang P, Li R. Photocatalytic degradation of methylene blue in ZIF-8. *RSC Adv.* 2014; 4(97): 54454–54462.

Received 2024-01-05
Accepted 2024-03-28